On the Relation Between Grey and White Tin (α-Sn and β-Sn)
Author(s): M. J. P. Musgrave
Source: *Proceedings of the Royal Society of London. Series A, Mathematical and Physical Sciences*, Vol. 272, No. 1351 (Apr. 9, 1963), pp. 503-528
Published by: The Royal Society
Stable URL: http://www.jstor.org/stable/2414385
Accessed: 02/07/2010 13:03

On the relation between grey and white tin (α-Sn and β-Sn)

By M. J. P. Musgrave

Basic Physics Division, National Physical Laboratory, Teddington, Middlesex

(*Communicated by J. A. Pople, F.R.S.—Received* 30 *August* 1962)

A model capable of representing the structure of either grey or white tin and susceptible to lattice dynamical analysis has been studied. Values of atomic force constants for the models have been estimated and used in the appropriate secular equations to calculate frequency distributions of lattice modes for the two phases. From these distributions, thermodynamic quantities (in particular the specific heat and the vibrational contribution to the free energy) have been computed and the results are compared with observed data; fair agreement is found in view of the assumptions involved and the lack of any observed elastic constants for grey tin.

The values of the force constants in relation to the phase change are discussed and a suggestion about the interpretation of the angular stiffnesses in terms of the interaction of the Fermi surface with Brillouin polyhedra is offered.

1. Introduction

Tin is commonly found in one of two allotropic forms, α-Sn having the diamond structure, or β-Sn having a body-centred tetragonal structure. It is possible to regard the α-phase also as a body-centred tetragonal structure have a particular value of the axial ratio which gives rise to the higher cubic symmetry. As has been pointed out by Hall (1956), Prasad & Wooster (1956), and more recently by Miasek & Suffczynski (1961), the β-phase may then be interpreted as a structure in which the regular tetrahedral assemblage of first neighbours is distorted by a shear, which enlarges by equal amounts the two angles in the planes of symmetry containing the z axis ($\theta \rightarrow \phi'$) and correspondingly decreases the remaining four ($\theta \rightarrow \phi$), while the first-neighbour distances are equally extended by a small amount (see figures 1 and 2).

It seems at least possible that the actual transition from the α- to the β-phase could take this mechanical path. Wolfson, Fine & Ewald (1960) report that 'the gray tin buckles visibly immediately in front of the advancing interface' (of transformation from α-Sn to β-Sn). Accordingly, a lattice dynamical model of the structure with arbitrary axial ratio has been set up with the purpose of relating the central and angular stiffnesses assumed for the model to the elastic constants of the crystal. The determination of such force constants for the β-Sn structure allows a calculation of the frequency distribution and hence various thermodynamic quantities. In the absence of a set of observed elastic constants for α-Sn, an estimate of appropriate force constants has been made and a frequency distribution and thermodynamic quantities computed for comparison with the β-phase and experimental observations.

An interpretation of the negative values of some of the angular stiffnesses is offered and their possible relevance to the mode of instability indicated.

2. Specification of the β-Sn structure

Diamond structure has already been numbered by Musgrave & Pople (1962) in dealing with a general valence force field and it is convenient here to use the same enumeration while referring to x' and y' tetragonal axes having directions $(1, 1, 0)$ and $(\bar{1}, 1, 0)$ when referred to the cubic axes x and y of the diamond structure. Figures 1 and 2 and table 1 together specify the reference atoms and neighbours which will be considered in this work.

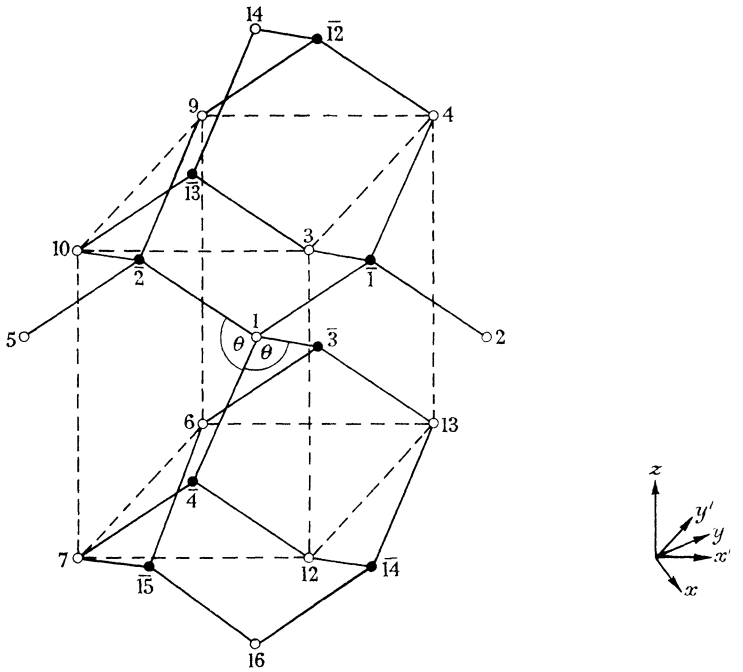

Figure 1. The diamond structure of grey tin (α-Sn) as interlinked body-centred tetragonal lattices with $\rho = c/2a' = 1/\sqrt{2}$. Numbering of atoms in accordance with table 1.

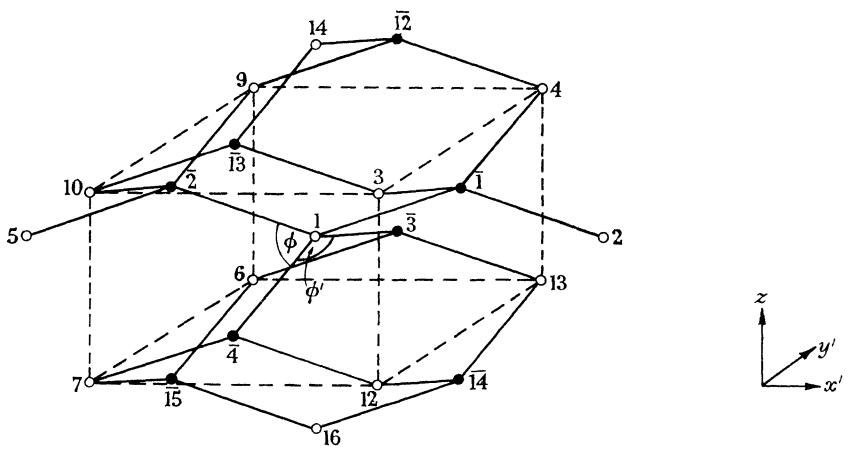

Figure 2. The structure of white tin (β-Sn) as interlinked body-centred tetragonal lattices with $\rho = c/2a' = 0{\cdot}272$. Numbering of atoms in accordance with table 1.

The atomic dimensions and elastic constants of β-Sn have been determined at various temperatures from 4·2 to 300 °K by Rayne & Chandrasekhar (1960) and their values of the atomic spacings are given in table 2 together with values of the spacings in α-Sn due to Wyckoff (1948).

TABLE 1. SPECIFICATION OF ATOMS IN α-Sn AND β-Sn STRUCTURES

The co-ordinates of each atom are given with reference to (i) the usual cube axes of diamond structure, and (ii) the tetragonal axes of β-Sn structure. When the axial ratio $\rho = c/2a' = 1/\sqrt{2}$, the β-Sn structure is identical with the diamond structure.

	co-ordinates referred to cube axes of diamond structure (units)			co-ordinates referred tetragonal axes of β-Sn (units)			class of neighbour	
no. of atom	a	a	a	a'	a'	c	in α-Sn	in β-Sn
1	0	0	0	0	0	0	—	—
2	1	1	0	1	0	0	2 (12)	6 (4)
3	1	0	1	$\frac{1}{2}$	$-\frac{1}{2}$	$\frac{1}{2}$	2	4 (8)
4	0	1	1	$\frac{1}{2}$	$\frac{1}{2}$	$\frac{1}{2}$	2	4
5	$\bar{1}$	$\bar{1}$	0	$\bar{1}$	0	0	2	6
6	$\bar{1}$	0	$\bar{1}$	$-\frac{1}{2}$	1	$-\frac{1}{2}$	2	4
7	0	$\bar{1}$	$\bar{1}$	$-\frac{1}{2}$	$-\frac{1}{2}$	$-\frac{1}{2}$	2	4
8	$\bar{1}$	1	0	0	1	0	2	6
9	$\bar{1}$	0	1	$-\frac{1}{2}$	$\frac{1}{2}$	$\frac{1}{2}$	2	4
10	0	$\bar{1}$	1	$-\frac{1}{2}$	$-\frac{1}{2}$	$\frac{1}{2}$	2	4
11	1	$\bar{1}$	0	0	$\bar{1}$	0	2	6
12	1	0	$\bar{1}$	$\frac{1}{2}$	$-\frac{1}{2}$	$-\frac{1}{2}$	2	4
13	0	1	$\bar{1}$	$\frac{1}{2}$	$\frac{1}{2}$	$-\frac{1}{2}$	2	4
14	0	0	2	0	0	1	4 (6)	2 (2)
15	1	1	2	1	0	1	—	—
16	0	0	$\bar{2}$	0	0	$\bar{1}$	4	2
$\bar{1}$	$\frac{1}{2}$	$\frac{1}{2}$	$\frac{1}{2}$	$\frac{1}{2}$	0	$\frac{1}{4}$	1 (4)	1 (4)
$\bar{2}$	$-\frac{1}{2}$	$-\frac{1}{2}$	$\frac{1}{2}$	$-\frac{1}{2}$	0	$\frac{1}{4}$	1	1
$\bar{3}$	$-\frac{1}{2}$	$\frac{1}{2}$	$-\frac{1}{2}$	0	$\frac{1}{2}$	$-\frac{1}{4}$	1	1
$\bar{4}$	$\frac{1}{2}$	$-\frac{1}{2}$	$-\frac{1}{2}$	0	$-\frac{1}{2}$	$-\frac{1}{4}$	1	1
$\bar{5}$	$\frac{3}{2}$	$\frac{3}{2}$	$\frac{1}{2}$	$\frac{3}{2}$	0	$\frac{1}{4}$	—	—
$\bar{6}$	$\frac{3}{2}$	$\frac{1}{2}$	$\frac{3}{2}$	1	$-\frac{1}{2}$	$\frac{3}{4}$	—	—
$\bar{7}$	$\frac{1}{2}$	$\frac{3}{2}$	$\frac{3}{2}$	1	$\frac{1}{2}$	$\frac{3}{4}$	—	—
$\bar{8}$	$\frac{3}{2}$	$-\frac{1}{2}$	$\frac{1}{2}$	$\frac{1}{2}$	-1	$\frac{1}{4}$	3 (8)	—
$\bar{9}$	$\frac{3}{2}$	$\frac{1}{2}$	$-\frac{1}{2}$	1	$-\frac{1}{2}$	$-\frac{1}{4}$	3	—
$\bar{10}$	$\frac{1}{2}$	$\frac{3}{2}$	$-\frac{1}{2}$	1	$\frac{1}{2}$	$-\frac{1}{4}$	3	—
$\bar{11}$	$-\frac{1}{2}$	$\frac{3}{2}$	$\frac{1}{2}$	$\frac{1}{2}$	1	$\frac{1}{4}$	3	—
$\bar{12}$	$-\frac{1}{2}$	$\frac{1}{2}$	$\frac{3}{2}$	0	$\frac{1}{2}$	$\frac{3}{4}$	3	3 (4)
$\bar{13}$	$\frac{1}{2}$	$-\frac{1}{2}$	$\frac{3}{2}$	0	$-\frac{1}{2}$	$\frac{3}{4}$	3	3
$\bar{14}$	$\frac{1}{2}$	$\frac{1}{2}$	$-\frac{3}{2}$	$\frac{1}{2}$	0	$-\frac{3}{4}$	3	3
$\bar{15}$	$-\frac{1}{2}$	$-\frac{1}{2}$	$-\frac{3}{2}$	$-\frac{1}{2}$	0	$-\frac{3}{4}$	3	3
$\bar{16}$	$\frac{1}{2}$	$\frac{1}{2}$	$\frac{5}{2}$	$\frac{1}{2}$	0	$\frac{5}{4}$	—	5 (4)

Note. The number of neighbours of a given class in each structure is given in brackets by the first-listed member of each class.

To assess the significance of the interactions between the various sets of neighbours is one of the main purposes of this essay; however, since there are only six independent elastic constants from which to derive atomic force constants, progress is not possible without some extensive simplifications. First, let us glimpse at what

the retention of generality would demand and derive the number of independent force constants for the various sets of neighbours by using the symmetry elements of the structure in the context of Born's lattice dynamics.

TABLE 2. ATOMIC DIMENSIONS OF α-Sn AND β-Sn (300 °K)

α-Sn			β-Sn		
class of neighbour	distance	Å	class of neighbour	distance ($\rho = c/2a'$)	Å
1	$\frac{1}{2}a\sqrt{3}$	2·80	1	$\frac{1}{2}a'(1+\rho^2)^{\frac{1}{2}}$	3·0224
2	$a\sqrt{2}$	4·59	2	c	3·1828
3	$\frac{1}{2}a\sqrt{11}$	5·38	3	$\frac{1}{2}a'(1+9\rho^2)^{\frac{1}{2}}$	3·7682
4	$2a$	6·49	4	$(1/\sqrt{2})\,a'(1+2\rho^2)^{\frac{1}{2}}$	4·4122
density = 5·75 g/cm³			5	$\frac{1}{2}a'(1+25\rho^2)^{\frac{1}{2}}$	4·9324
			6	a'	5·8315
			density = 7·31 g/cm³		

3. GENERAL FORCE CONSTANTS FOR THE β-Sn STRUCTURE

The following operations specify the group:

(1) reflexion in the plane $x' = 0$, $T_1 = \begin{bmatrix} \bar{1} & 0 & 0 \\ 0 & 1 & 0 \\ 0 & 0 & 1 \end{bmatrix}$;

(2) reflexion in the plane $y' = 0$, $T_2 = \begin{bmatrix} 1 & 0 & 0 \\ 0 & \bar{1} & 0 \\ 0 & 0 & 1 \end{bmatrix}$;

(3) reflexion in planes $x' = \pm y'$ followed by reflexion in $z = 0$, $T_3 = \begin{bmatrix} 0 & 1 & 0 \\ 1 & 0 & 0 \\ 0 & 0 & \bar{1} \end{bmatrix}$;

$T_4 = \begin{bmatrix} 0 & \bar{1} & 0 \\ \bar{1} & 0 & 0 \\ 0 & 0 & \bar{1} \end{bmatrix}$;

(4) inversion about $(\frac{1}{4}a', 0, \frac{1}{8}c)$, i.e. reflexion in the origin followed by a translation, $T_5 = \begin{bmatrix} \bar{1} & 0 & 0 \\ 0 & \bar{1} & 0 \\ 0 & 0 & \bar{1} \end{bmatrix}$.

Denoting by $-\Phi_{\alpha\beta}(l, l')$, the force on l in direction α caused by unit displacement of l' in direction β, and applying the above operations, we find $\Phi_{\alpha\beta}$ typical of the first six sets of neighbours as follows:

$$\Phi_{\alpha\beta}(1, \bar{3}) = -\begin{bmatrix} \alpha & 0 & 0 \\ 0 & \beta & \gamma \\ 0 & \gamma' & \beta' \end{bmatrix} \quad \text{representative of first neighbours,}$$

$$\Phi_{\alpha\beta}(1, 14) = -\begin{bmatrix} \delta & 0 & 0 \\ 0 & \delta' & 0 \\ 0 & 0 & \delta'' \end{bmatrix} \quad \text{representative of second neighbours,}$$

$$\Phi_{\alpha\beta}(1,\overline{13}) = -\begin{bmatrix}\lambda & 0 & 0\\ 0 & \mu & \nu\\ 0 & \nu' & \mu'\end{bmatrix} \quad \text{representative of third neighbours,}$$

$$\Phi_{\alpha\beta}(1,3) = -\begin{bmatrix}\rho & \omega & \tau\\ \omega' & \rho' & \sigma\\ \tau' & \sigma' & \rho''\end{bmatrix} \quad \text{representative of fourth neighbours,}$$

$$\Phi_{\alpha\beta}(1,\overline{16}) = -\begin{bmatrix}\kappa' & 0 & \chi\\ 0 & \kappa & 0\\ \chi' & 0 & \kappa''\end{bmatrix} \quad \text{representative of fifth neighbours,}$$

$$\Phi_{\alpha\beta}(1,2) = -\begin{bmatrix}\zeta & 0 & \eta\\ 0 & \zeta' & 0\\ \eta' & 0 & \zeta''\end{bmatrix} \quad \text{representative of sixth neighbours.}$$

The dynamical matrices for the other neighbours may all be found from those above by application of the symmetry elements; those used in the sequel are listed in appendix 1. The total number of force constants necessary to represent general interaction up to sixth neighbours is 32. Consequently, an intuitive choice of atomic stiffnesses likely to be significant is the only viable approach.

4. Choice of a force field for the β-Sn structure

The elastic constants of carbon, silicon and germanium may, to a first approximation, be successfully interpreted in terms of a simple valence force field consisting of an extensional stiffness between nearest neighbours, k_r and an angular stiffness, k_θ. Consequently it seems appropriate to attempt to extend these concepts to the β-Sn structure. The more complicated model should of course simplify to the elementary form of valence force field when $\rho = 1/\sqrt{2}$ as in α-Sn.

In the β-Sn structure, the six angles formed at the centre of the tetrahedral assemblage $1\,\overline{1}\,\overline{2}\,\overline{3}\,\overline{4}$ consist of a four and a pair of different magnitudes, ϕ and ϕ', as shown in figure 2. We assume two different angular stiffnesses k_ϕ and $k_{\phi'}$, associated with the deformations of these two types of angle; further, the second and third neighbours are much nearer so that central stiffnesses k_1, k_2, k_3 would seem essential. We may now choose one more force constant determinable from six elastic constants. The introduction of central stiffnesses k_4 or k_6 gives rise to a partial redundance since they are already to some extent implied by k_ϕ and $k_{\phi'}$, so k_5 is the most obvious candidate among central stiffnesses. On the other hand, if the transition occurs in the mode here envisaged, deformation of the angles in the structure may very probably be more important than the change of fifth neighbour spacing and a further constant relating to angular deformation may prove to be of greater relevance. It would also have the advantage that any further interpretation could include concepts which are not localized but pertain to the crystal structure as a whole, namely the band structure in relation to the Brillouin polyhedra. Pursuing this intuition, some form of interaction constant for deformations of the angles ϕ and/or ϕ' seems appropriate. Since the change in magnitude of ϕ' in the transition from the α- to the β-form is much greater than that of ϕ, it is perhaps reasonable

to suppose that an interaction constant, $k_{\phi'\phi'}$, for deformations of opposite angles ϕ', may prove an interesting choice for the sixth force constant.

A model in which the stiffnesses k_1, k_2, k_3, k_ϕ, $k_{\phi'}$, $k_{\phi'\phi'}$ are preferentially significant is therefore proposed.

The potential energy of deformation is then

$$\Phi = \tfrac{1}{2}k_1 \sum_{\text{1st neighbours}} (\delta r_{ij})^2 + \tfrac{1}{2}k_2 \sum_{\text{2nd neighbours}} (\delta r_{ij})^2 + \tfrac{1}{2}k_3 \sum_{\text{3rd neighbours}} (\delta r_{ij})^2 + \tfrac{1}{2}k_\phi r_0^2 \sum_{\text{all } \phi} (\delta\phi)^2 + \tfrac{1}{2}k_{\phi'} r_0^2 \sum_{\text{all } \phi'} (\delta\phi')^2 + k_{\phi'\phi'} r_0^2 \sum_{\text{opp. angles } \phi'} (\delta\phi')(\delta\phi'). \quad (4{\cdot}1)$$

5. Calculation of the contributions to the $\Phi_{\alpha\beta}$

The contributions to the $\Phi_{\alpha\beta}$ from the various constants of the assumed force field are determined as follows:

$$\Phi_{\alpha\beta}^{(r)}(1,n) = k_N \left[\frac{\partial r_{1n}}{\partial x_\alpha(1)}\right]_0 \left[\frac{\partial r_{1n}}{\partial x_\beta(n)}\right]_0, \quad (5{\cdot}1)$$

where n may specify any atom 2 to 16, $\bar{1}$ to $\bar{15}$ and N denotes the class of neighbour to which n belongs; if we write $r_0^2 = \frac{1}{4}a'^2(1+\rho^2)$, then

$$\Phi_{\alpha\beta}^{(\phi)}(1,n) = k_\phi r_0^2 \left\{ \left[\frac{\partial \phi_{1nm}}{\partial x_\alpha(1)}\right]_0 \left[\frac{\partial \phi_{1nm}}{\partial x_\beta(n)}\right]_0 + \left[\frac{\partial \phi_{m1n}}{\partial x_\alpha(1)}\right]_0 \left[\frac{\partial \phi_{m1n}}{\partial x_\beta(n)}\right]_0 \right\}, \quad (5{\cdot}2)$$

when $n = \bar{1}, \bar{2}, \bar{3}, \bar{4}$ and the sum over all appropriate m is taken in each case;

$$\Phi_{\alpha\beta}^{(\phi)}(1,n) = k_\phi r_0^2 \left\{ \left[\frac{\partial \phi_{1mn}}{\partial x_\alpha(1)}\right]_0 \left[\frac{\partial \phi_{1mn}}{\partial x_\beta(n)}\right]_0 \right\}, \quad (5{\cdot}3)$$

when $n = 3, 4, 6, 7, 9, 10, 12, 13$ and the appropriate m is chosen in each case; similar expressions to (5·2) and (5·3) determine $\Phi_{\alpha\beta}^{(\phi')}(1,n)$; finally

$$\Phi_{\alpha\beta}^{(\phi'\phi')}(1,n) = k_{\phi'\phi'} r_0^2 \left\{ \left[\frac{\partial \phi'_{1nm}}{\partial x_\alpha(1)}\right]_0 \left[\frac{\partial \phi'_{knl}}{\partial x_\beta(n)}\right]_0 + \left[\frac{\partial \phi'_{i1j}}{\partial x_\alpha(1)}\right]_0 \left[\frac{\partial \phi_{n1p}}{\partial x_\beta(n)}\right]_0 \right\}, \quad (5{\cdot}4)$$

when $n = \bar{1}, \bar{2}, \bar{3}, \bar{4}$ and

$$\Phi_{\alpha\beta}^{(\phi'\phi')}(1,n) = k_{\phi'\phi'} r_0^2 \left\{ \left[\frac{\partial \phi'_{1mp}}{\partial x_\alpha(1)}\right]_0 \left[\frac{\partial \phi'_{nmq}}{\partial x_\beta(n)}\right]_0 \right\}, \quad (5{\cdot}5)$$

when $n = 3, 4, 6, 7, 9, 10, 12, 13$, and in each case the remaining suffixes are chosen to yield opposite angles ϕ'.

The values of the partial derivatives in the above expressions are given by the following relations

$$\left[\frac{\partial r_{1n}}{\partial x_\gamma(1)}\right]_0 = \frac{x_\gamma(1) - x_\gamma(n)}{r_0} = -\left[\frac{\partial r_{1n}}{\partial x_\gamma(n)}\right]_0, \quad (5{\cdot}6)$$

$$\left[\frac{\partial \phi_{1nm}}{\partial x_\alpha(1)}\right]_0 = \frac{1}{r_0^2}[\{x_\alpha(1) - x_\alpha(n)\}\cot\phi_0 - \{x_\alpha(m) - x_\alpha(n)\}\operatorname{cosec}\phi_0], \quad (5{\cdot}7)$$

$$\left[\frac{\partial \phi_{1nm}}{\partial x_\beta(n)}\right]_0 = \frac{1}{r_0^2}[\{x_\beta(1) - x_\beta(n)\} - \{x_\beta(n) - x_\beta(m)\}][\operatorname{cosec}\phi_0 - \cot\phi_0], \quad (5{\cdot}8)$$

where $$\cot\phi_0 = \frac{-\rho^2}{\sqrt{(1+2\rho^2)}}, \quad \operatorname{cosec}\phi_0 = \frac{1+\rho^2}{\sqrt{(1+2\rho^2)}}$$

so that
$$\operatorname{cosec}\phi_0 - \cot\phi_0 = \sqrt{(1+2\rho^2)},$$
$$\operatorname{cosec}\phi_0 + \cot\phi_0 = \frac{1}{\sqrt{(1+2\rho^2)}}, \tag{5·9}$$

and
$$\left[\frac{\partial\phi'_{1mn}}{\partial x_\alpha(1)}\right]_0 = \frac{1}{r_0^2}[\{x_\alpha(1)-x_\alpha(m)\}\cot\phi'_0 - \{x_\alpha(n)-x_\alpha(m)\}\operatorname{cosec}\phi'_0], \tag{5·10}$$

$$\left[\frac{\partial\phi'_{1mn}}{\partial x_\beta(n)}\right]_0 = \frac{1}{r_0^2}[\{x_\beta(n)-x_\beta(m)\}\cot\phi'_0 - \{x_\beta(1)-x_\beta(m)\}\operatorname{cosec}\phi'_0], \tag{5·11}$$

where
$$\cot\phi'_0 = -(1-\rho^2)/2\rho, \quad \operatorname{cosec}\phi'_0 = (1+\rho^2)/2\rho, \tag{5·12}$$

so that $\operatorname{cosec}\phi'_0 \pm \cot\phi'_0 = \rho^{\pm 1}$.

Using relations (5·1) to (5·12), we find that the contributions to the $\Phi_{\alpha\beta}$ for atoms representative of each class of neighbour have the following forms:

$$\Phi_{\alpha\beta}(1,\bar{1}) = -\frac{k_1}{1+\rho^2}\begin{bmatrix}1&0&\rho\\0&0&0\\\rho&0&\rho^2\end{bmatrix} - \frac{2k_\phi}{1+\rho^2}\begin{bmatrix}2\rho^2&0&-\rho\\0&2(1+\rho^2)&0\\-\rho&0&0\end{bmatrix} - \frac{2(k_{\phi'}-k_{\phi'\phi'})}{1+\rho^2}\begin{bmatrix}0&0&-\rho\\0&0&0\\-\rho&0&2\end{bmatrix}, \tag{5·13}$$

$$\Phi_{\alpha\beta}(1,14) = -k_2\begin{bmatrix}0&0&0\\0&0&0\\0&0&1\end{bmatrix}, \tag{5·14}$$

$$\Phi_{\alpha\beta}(1,\overline{14}) = -\frac{k_3}{1+9\rho^2}\begin{bmatrix}1&0&-3\rho\\0&0&0\\-3\rho&0&9\rho^2\end{bmatrix}, \tag{5·15}$$

$$\Phi_{\alpha\beta}(1,3) = \frac{k_\phi}{(1+\rho^2)(1+2\rho^2)}\begin{bmatrix}\rho^2(1+\rho^2)&\rho^4&\rho^3\\(1+\rho^2)^2&\rho^2(1+\rho^2)&\rho(1+\rho^2)\\-\rho(1+\rho^2)&-\rho^3&-\rho^2\end{bmatrix} + \frac{k_{\phi'\phi'}}{1+\rho^2}\begin{bmatrix}0&\rho^2&\rho\\0&0&0\\0&-\rho&-1\end{bmatrix}, \tag{5·16}$$

$$\Phi_{\alpha\beta}(1,2) = -\frac{k_{\phi'}}{1+\rho^2}\begin{bmatrix}\rho^2&0&\rho\\0&0&0\\-\rho&0&-1\end{bmatrix}. \tag{5·17}$$

When $\rho = 1/\sqrt{2}$ and $k_2 = 0 = k_3 = k_{\phi'\phi'}$, $k_\phi = k_{\phi'}$, these reduce to the matrices for a simple valence force field in diamond structure referred to tetragonal axes.

6. The equations of motion and the frequency equation

The equations of motion for the two reference atoms 1 and $\bar{1}$ may now be written down and the plane wave displacements

$$u_\alpha(1)\exp i\omega\{q_\alpha x'_\alpha(n) - t\}, \quad \bar{u}_\alpha(\bar{1})\exp i\omega\{q_\alpha x'_\alpha(\bar{n}) - t\}$$

for each Bravais lattice of the structure may be substituted therein; the vectors u_α (displacement), q_α (slowness), x'_α (position) have components parallel to x', y', z axes as $\alpha = 1, 2, 3$. The six simultaneous equations

$$\begin{bmatrix} F-\Lambda & J & K & P & 0 & C \\ J^* & G-\Lambda & L & 0 & Q & D \\ K^* & L^* & H-\Lambda & C & D & R \\ P^* & 0 & C^* & F-\Lambda & J^* & K^* \\ 0 & Q^* & D^* & J & G-\Lambda & L^* \\ C^* & D^* & R^* & K & L & H-\Lambda \end{bmatrix} \begin{bmatrix} u_1(1) \\ u_2(1) \\ u_3(1) \\ \bar{u}_1(\bar{1}) \\ \bar{u}_2(\bar{1}) \\ \bar{u}_3(\bar{1}) \end{bmatrix} = 0 \tag{6·1}$$

are then obtained, where $\Lambda = m\omega^2$, m being the mass of the constituent atom. The spectrum of angular frequencies $\omega_i(q_\alpha)$ $(i = 1, 2, \ldots, 6)$, is obtained from the latent roots of the 6×6 matrix and the corresponding vectors may thence be found.

The elements of the matrix in expanded form are

$$F = \frac{2[k_1 + 4\rho^2 k_\phi]}{1+\rho^2} + 8k_\phi + \frac{2k_3}{1+9\rho^2} - \frac{8\rho^2 k_\phi}{1+2\rho^2}[1 - \cos\tfrac{1}{2}q_1 a' \cos\tfrac{1}{2}q_2 a' \cos\tfrac{1}{2}q_3 c] + \frac{2\rho^2 k_{\phi'}}{1+\rho^2}[1 - \cos q_1 a'], \tag{6·2}$$

$$G = \frac{2[k_1 + 4\rho^2 k_\phi]}{1+\rho^2} + 8k_\phi + \frac{2k_3}{1+9\rho^2} - \frac{8\rho^2 k_\phi}{1+2\rho^2}[1 - \cos\tfrac{1}{2}q_1 a' \cos\tfrac{1}{2}q_2 a' \cos\tfrac{1}{2}q_3 c] + \frac{2\rho^2 k_{\phi'}}{1+\rho^2}[1 - \cos q_2 a'], \tag{6·3}$$

$$H = \frac{4[\rho^2 k_1 + 4(k_{\phi'} - k_{\phi'\phi'})]}{1+\rho^2} + 2k_2[1 - \cos q_3 c] + \frac{36\rho^2 k_3}{1+9\rho^2} + \frac{8}{1+\rho^2}\left\{\frac{\rho^2 k_\phi}{1+2\rho^2} + k_{\phi'\phi'}\right\}[1 - \cos\tfrac{1}{2}q_1 a' \cos\tfrac{1}{2}q_2 a' \cos\tfrac{1}{2}q_3 c] - \frac{2k_{\phi'}}{1+\rho^2}[2 - \cos q_1 a' - \cos q_2 a'], \tag{6·4}$$

$$J = 4\left[\frac{k_\phi}{1+2\rho^2}\left\{\frac{\rho^4}{1+\rho^2}\mathrm{e}^{\frac{1}{2}\mathrm{i}q_3 c} + (1+\rho^2)\mathrm{e}^{-\frac{1}{2}\mathrm{i}q_3 c}\right\} + \frac{\rho^2}{1+\rho^2}k_{\phi'\phi'}\mathrm{e}^{\frac{1}{2}\mathrm{i}q_3 c}\right]\sin\tfrac{1}{2}q_1 a' \sin\tfrac{1}{2}q_2 a', \tag{6·5}$$

$$K = -\mathrm{i}\left[\frac{2\rho}{1+\rho^2}k_{\phi'}\sin q_1 a' - 4\rho\left\{\frac{\rho^2 k_\phi \mathrm{e}^{\frac{1}{2}\mathrm{i}q_3 c}}{(1+\rho^2)(1+2\rho^2)} + \frac{k_{\phi'\phi'}\mathrm{e}^{\frac{1}{2}\mathrm{i}q_3 c}}{1+\rho^2} + \frac{k_\phi \mathrm{e}^{-\frac{1}{2}\mathrm{i}q_3 c}}{1+2\rho^2}\right\}\sin\tfrac{1}{2}q_1 a' \cos\tfrac{1}{2}q_2 a'\right], \tag{6·6}$$

$$L = -\mathrm{i}\left[\frac{2\rho}{1+\rho^2}k_{\phi'}\sin q_2 a' - 4\rho\left\{\frac{\rho^2 k_\phi \mathrm{e}^{\frac{1}{2}\mathrm{i}q_3 c}}{(1+\rho^2)(1+2\rho^2)} + \frac{k_{\phi'\phi'}\mathrm{e}^{\frac{1}{2}\mathrm{i}q_3 c}}{1+\rho^2} + \frac{k_\phi \mathrm{e}^{-\frac{1}{2}\mathrm{i}q_3 c}}{1+2\rho^2}\right\}\cos\tfrac{1}{2}q_1 a' \sin\tfrac{1}{2}q_2 a'\right], \tag{6·7}$$

$$C = -\mathrm{i}\left[\frac{2\rho}{1+\rho^2}\{k_1 - 2(k_\phi + \overline{k_{\phi'} - k_{\phi'\phi'}})\}\,\mathrm{e}^{\frac{1}{4}\mathrm{i}q_3 c} - \frac{6\rho k_3\,\mathrm{e}^{-\frac{1}{4}\mathrm{i}3q_3 c}}{1+9\rho^2}\right]\sin\tfrac{1}{2}q_1 a', \tag{6·8}$$

$$D = +\mathrm{i}\left[\frac{2\rho}{1+\rho^2}\{k_1 - 2(k_\phi + \overline{k_{\phi'} - k_{\phi'\phi'}})\}\,\mathrm{e}^{-\frac{1}{4}\mathrm{i}q_3 c} - \frac{6\rho k_3\,\mathrm{e}^{\frac{1}{4}\mathrm{i}3q_3 c}}{1+9\rho^2}\right]\sin\tfrac{1}{2}q_2 a', \tag{6·9}$$

$$P = -2\left[\left\{\frac{k_1 + 4\rho^2 k_\phi}{1+\rho^2}\right\}\cos\tfrac{1}{2}q_1 a'\,\mathrm{e}^{\frac{1}{4}\mathrm{i}q_3 c} + 4k_\phi\cos\tfrac{1}{2}q_2 a'\,\mathrm{e}^{-\frac{1}{4}\mathrm{i}q_3 c} + \frac{k_3}{1+9\rho^2}\cos\tfrac{1}{2}q_1 a'\,\mathrm{e}^{-\frac{1}{4}\mathrm{i}3q_3 c}\right], \tag{6·10}$$

$$Q = -2\left[\left\{\frac{k_1 + 4\rho^2 k_\phi}{1+\rho^2}\right\}\cos\tfrac{1}{2}q_2 a'\,\mathrm{e}^{-\frac{1}{4}\mathrm{i}q_3 c} + 4k_\phi\cos\tfrac{1}{2}q_1 a'\,\mathrm{e}^{\frac{1}{4}\mathrm{i}q_3 c} + \frac{k_3}{1+9\rho^2}\cos\tfrac{1}{2}q_2 a'\,\mathrm{e}^{\frac{1}{4}\mathrm{i}3q_3 c}\right], \tag{6·11}$$

$$R = -2\left[\left\{\frac{\rho^2 k_1 + 4\overline{k_{\phi'} - k_{\phi'\phi'}}}{1+\rho^2}\right\}\{\cos\tfrac{1}{2}q_1 a'\,\mathrm{e}^{\frac{1}{4}\mathrm{i}q_3 c} + \cos\tfrac{1}{2}q_2 a'\,\mathrm{e}^{-\frac{1}{4}\mathrm{i}q_3 c}\} + \frac{9\rho^2 k_3}{1+9\rho^2}\{\cos\tfrac{1}{2}q_1 a'\,\mathrm{e}^{-\frac{1}{4}\mathrm{i}3q_3 c} + \cos\tfrac{1}{2}q_2 a'\,\mathrm{e}^{\frac{1}{4}\mathrm{i}3q_3 c}\}\right]. \tag{6·12}$$

7. The relation between the elastic constants and the force constants

In the limit as $q \to 0$ and $\omega \to 0$, $\omega/q = v$, the phase velocity of elastic waves in the medium; hence we obtain relations between the elastic constants and the atomic force constants.

The expansions in powers of the components q_α of the elements of the matrix are, to second order,

$$\left.\begin{aligned}
F &= F_0 && + F_2(q_1^2, q_2^2, q_3^2, q_2q_3, q_3q_1, q_1q_2)\\
G &= G_0 && + G_2\\
H &= H_0 && + H_2\\
J &= && J_2\\
K &= & K_1(q_1, q_2, q_3) & + K_2\\
L &= & L_1 & + L_2\\
P &= P_0 + P_1 && + P_2\\
Q &= Q_0 + Q_1 && + Q_2\\
R &= R_0 && + R_2\\
C &= & C_1 & + C_2\\
D &= & D_1 & + D_2
\end{aligned}\right\} \tag{7·1}$$

Following the arguments of Born (see, for instance, Born & Huang 1956) the relative displacement of the reference atoms may be determined to the first order from the equation

$$\begin{bmatrix} P_0 & 0 & 0\\ 0 & Q_0 & 0\\ 0 & 0 & R_0 \end{bmatrix}\begin{bmatrix} u_\alpha^{(1)}(1) - \bar{u}_\alpha^{(1)}(\bar{1}) \end{bmatrix} + \begin{bmatrix} P_1 & 0 & C_1 + K_1\\ 0 & Q_1 & D_1 + L_1\\ C_1 - K_1 & D_1 - L_1 & 0 \end{bmatrix}\begin{bmatrix} u_\alpha(1) \end{bmatrix} = 0 \tag{7·2}$$

and then the frequency equation to second order in q may be obtained as

$$m\omega^2\begin{bmatrix} u_\alpha(1) \\ \\ \end{bmatrix} = \left\{ -\tfrac{1}{2}\begin{bmatrix} P_1 & 0 & C_1-K_1 \\ 0 & Q_1 & D_1-L_1 \\ C_1+K_1 & D_1+L_1 & 0 \end{bmatrix}\begin{bmatrix} P_1/P_0 & 0 & \overline{C_1+K_1}/P_0 \\ 0 & Q_1/Q_0 & \overline{D_1+L_1}/Q_0 \\ \overline{C_1-K_1}/R_0 & \overline{D_1-L_1}/R_0 & 0 \end{bmatrix} + \begin{bmatrix} F_2+P_2 & J_2 & C_2+K_2 \\ J_2 & G_2+Q_2 & D_2+L_2 \\ C_2+K_2 & D_2+L_2 & H_2+R_2 \end{bmatrix}\right\}\begin{bmatrix} u_\alpha(1) \\ \\ \end{bmatrix}. \quad (7{\cdot}3)$$

Noting now that the density $\rho_D = 4m/a'^2c$ and in the limit of small ω and q, ω/q becomes the phase velocity of elastic waves, we may derive expressions for the elastic constants in terms of the following combinations of the force constants:

$$c_{11} = \frac{4}{c}\left[\frac{A+B}{4}+\frac{\rho^2}{2}\{M+N+2T\}-E-\frac{\rho^2\{A-3B-4N\}^2}{8\{\rho^2(A+9B)+4N\}}\right], \quad (7{\cdot}4)$$

$$c_{12} = \frac{4}{c}\left[\frac{\rho^2 E}{1+\rho^2}+\frac{\rho^2}{2}(M-N)+\frac{\rho^2}{8}\frac{\{A-3B-4N\}^2}{\{\rho^2(A+9B)+4N\}}\right], \quad (7{\cdot}5)$$

$$c_{13} = \frac{4}{c}\left[\frac{\rho^2}{4}(A+9B)+\frac{E}{1+\rho^2}-\rho^2(M+T)\right], \quad (7{\cdot}6)$$

$$c_{33} = \frac{4}{c}\left[\frac{\rho^4}{2}(A+81B)+4\rho^2 k_2+\frac{4\rho^2 E}{1+\rho^2}+2\rho^2 M\right], \quad (7{\cdot}7)$$

$$c_{44} = \frac{4}{c}\left[-4\rho^2 E+\frac{4\rho^2\{k_\phi(A+B+4\rho^2 T)+B(A+4\rho^2 T)\}}{A+B+4\rho^2 T+4k_\phi}\right], \quad (7{\cdot}8)$$

$$c_{66} = (4/c)[-E+k_\phi], \quad (7{\cdot}9)$$

where

$$\left.\begin{aligned} A &= \frac{k_1}{1+\rho^2}, & B &= \frac{k_3}{1+9\rho^2}, \\ E &= \frac{\rho^2 k_\phi}{1+2\rho^2}, & T &= \frac{k_\phi}{1+\rho^2}, \\ M &= \frac{k_{\phi'}+k_{\phi'\phi'}}{1+\rho^2}, & N &= \frac{k_{\phi'}-k_{\phi'\phi'}}{1+\rho^2}, \\ &= \frac{k_{\phi'}^+}{1+\rho^2}, & &= \frac{k_{\phi'}^-}{1+\rho^2}. \end{aligned}\right\} \quad (7{\cdot}10)$$

Each of these reduces to the appropriate expressions for elastic constants of cubic symmetry when $\rho = 1/\sqrt{2}$ and only k_1, $k_\phi = k_{\phi'}$ are non-zero.

It is worth remarking that the constant associated with bulk or purely dilatational strain $(\epsilon, \epsilon, \epsilon)$ is

$$2c_{11}+2c_{12}+4c_{13}+c_{33} = (4/c)[\tfrac{1}{2}(1+\rho^2)k_1+4\rho^2 k_2+\tfrac{1}{2}(1+9\rho^2)k_3] \quad (7{\cdot}11)$$

and independent of the angular stiffness, while the constants associated with the shears $(\epsilon, -\epsilon, 0)$ and $(\frac{1}{2}\epsilon, \frac{1}{2}\epsilon, -\epsilon)$ are respectively

$$c_{11}-c_{12}=\frac{4}{c}\left[\frac{A+B}{4}+\rho^2 N-\frac{\rho^2}{4}\frac{\{A-3B-4N\}^2}{\{\rho^2(A+9B)+4N\}}\right] \tag{7·12}$$

and

$$c_{11}+c_{12}-4c_{13}+2c_{33}=\frac{4}{c}\left[\frac{A}{4}(1-2\rho^2)^2+8\rho^2 k_2+\frac{B}{4}(1-18\rho^2)^2+9\rho^2\left\{M+\frac{2E}{1+\rho^2}\right\}\right]. \tag{7·13}$$

8. Numerical values of the force constants and the frequency distribution for β-Sn

The relations (7·4) to (7·9) may be used to derive values of the force constants from observed values of the elastic constants. Thus k_ϕ may be obtained from (7·9); summation of (7·4), (7·5), (7·6) yields

$$c_{11}+c_{12}+c_{13}=[k_1+k_3]/c \tag{8·1}$$

which in conjunction with (7·8) gives k_1 and k_3; k_2 can then be found from (7·11) after which k_ϕ^+ and k_ϕ^-, as defined in (7·10), are obtainable from (7·6) and (7·12).

Table 3 shows the elastic constants of β-Sn as they have been reported by various authors. The corresponding force constants have been calculated but each set has proved to render the model of the structure unstable to certain lattice modes ($\sim 5\,\%$) when the secular equation has been solved for a population of 72 wave vectors whose extremities are uniformly distributed over the repeating sixteenth portion of the Brillouin zone. The instability of these modes is a result of the negative values of the angular stiffnesses, $k_{\phi'}$ and $k_{\phi'\phi'}$ which are sensitive to changes in c_{13} as the two sets of constants for 300 °K, derived from Rayne & Chandrasekhar's measured phase velocities, indicate. The behaviour of $k_{\phi'}$ and $k_{\phi'\phi'}$ is discussed in a later section, but their sensitivity suggests that only a small change in the elastic constants would yield a set of force constants which would render the model of the structure stable. Examination of the secular equation which yields the most negative root (see appendix 2) has suggested that if the magnitude of the negative angular stiffness $k_{\phi'}$ is sufficiently small, the model is stable to all lattice modes. Accordingly, the sets of stabilized force constants have been produced which offer agreement with the observations of Rayne & Chandrasekhar except for the value of c_{13}; this constant has a value which though lower than their measurement, is not at all unreasonable in view of the considerable scatter of the values variously reported (see table 3).

With the use of set (iii) of stabilized force constants, a frequency distribution (figure 3) has been derived from the solutions to the secular equation over a population of 72 wave vectors. This distribution has been used as a basis for the calculation of such thermodynamic quantities as the specific heat C_v, the characteristic temperature, Θ, and the vibrational contribution to the free energy as functions of temperature. These results for β-Sn, together with similar calculations for α-Sn, are discussed in relation to experimental data in § 10.

TABLE 3. ELASTIC CONSTANTS AND FORCE CONSTANTS OF β-Sn

T (°K)	c_{11}	c_{33}	c_{12}	c_{13}	c_{44}	c_{66}	k_1	k_2	k_3	k_ϕ	$k_{\phi'}$	$k_{\phi'\phi'}$	
4·2	8·274	10·310	5·785	3·421	2·695	2·818	4·243	2·621	1·276	0·240	−0·617	−0·430	Rayne & Chandrasekhar
77	8·152	10·040	5·790	3·642	2·620	2·781	4·436	2·811	1·123	0·235	−0·818	−0·652	Rayne & Chandrasekhar
300	7·23	8·84	5·940	3·578	2·203	2·400	4·364	2·648	0·953	0·204	−0·917	−0·740	Rayne & Chandrasekhar
300*	7·23	8·84	5·940	3·454	2·203	2·400	4·321	2·584	0·957	0·204	−0·848	−0·672	Rayne & Chandrasekhar
300	7·4	8·7	2·3	2·8	2·2	2·26	2·830	2·179	1·139	0·192	−0·518	−0·360	Mason & Bömmel
300†	7·6	9·7	6·2	4·4	2·2	2·3	4·742	3·175	1·037	0·195	−1·270	−1·112	House & Vernon
300†	8·4	9·7	4·9	2·8	1·75	0·74	4·299	2·629	0·813	0·063	−0·545	−0·430	Bridgman
300‡	8·6	13·3	3·5	3·0	4·9	5·3	—	—	—	—	—	—	Prasad & Wooster
	8·274	10·310	5·785	2·67	2·695	2·818	3·971	2·214	1·311	0·240	−0·196	$-0·005_3$	(i) stabilized force constants fitting R. & C.'s observations except for c_{13}
	8·152	10·040	5·790	2·50	2·620	2·781	4·034	2·204	1·165	0·235	−0·185	$-0·014_2$	(ii) stabilized force constants fitting R. & C.'s observations except for c_{13}
	7·23	8·84	5·940	2·25	2·203	2·400	3·905	1·955	0·991	0·204	−0·172	$-0·022_8$	(iii) stabilized force constants fitting R. & C.'s observations except for c_{13}

* c_{ij} at 300 °K but c_{13} calculated from velocities more directly than the method reported by Rayne & Chandrasekhar. The sensitivity of $k_{\phi'}$ and $k_{\phi'\phi'}$ is considerable, though their difference k_{ϕ}^{-} remains almost constant.

† c_{ij} obtained by inversion of measured s_{ij}.

‡ The solutions for k_1 and k_3 from (7·8) and (8·1) prove to be complex roots. The negative discriminant for the quadratic equation appears to be the result of the high values of the shear constants c_{44} and c_{66}.

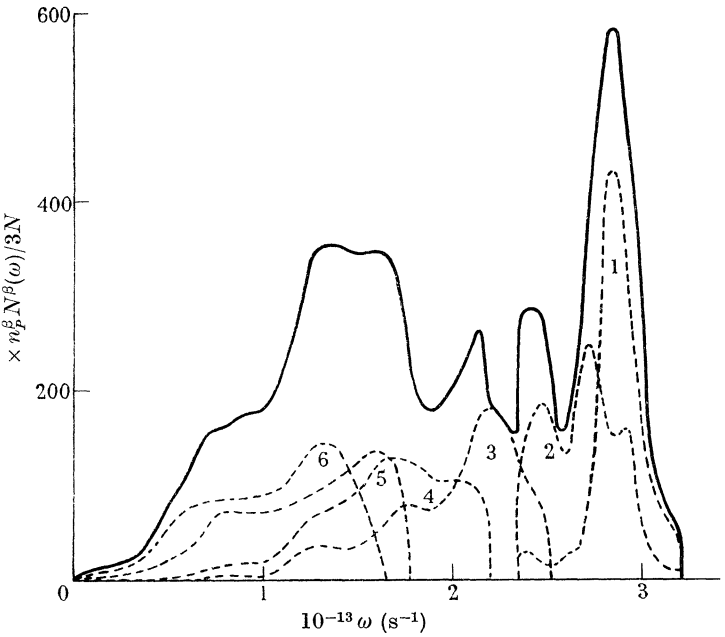

FIGURE 3. Calculated frequency distribution of lattice modes in β-Sn. n_p^β is the effective total population of calculated frequencies, $N^\beta(\omega)\,\Delta\omega$ is the number of frequencies per mole lying in the range $\Delta\omega$, N is Avogadro's number.

9. FORCE CONSTANTS, ELASTIC CONSTANTS AND THE FREQUENCY DISTRIBUTION FOR α-Sn

Grey tin occurs commonly in a powdery form and it is generally presumed that this fragmentation is related to the large decrease in density when the transition from white tin takes place. Single crystals of α-Sn have been prepared from an amalgam in recent years (see Ewald & Tufte 1958), but their size does not appear to have offered encouragement for a measurement of the three elastic constants.

The only values extant seem to be those suggested by Potter (1957) in the light of various thermal data. In view of this, it is perhaps justifiable to seek other guides as to their values in relation to the present work.

Examination of the observed elastic constants of other diamond structure elements shows that, to a first approximation, they are interpretable in terms of a simple valence force field represented by an extensional stiffness, k_r, and an angular stiffness, k_θ, where $k_r \sim 18k_\theta$. If we are prepared to accept this highly simplified model, then an estimate of a single elastic or force constant will serve to define the remainder.

It is possible to put some bounds on the values of k_r by plotting the values of the central force constants, k_1, k_2 and k_3 against corresponding atomic spacings and then extrapolating the exponential-like curve which may be drawn through them (figure 4). Assuming that the same force law is operative for all three constants of β-Sn and for first neighbours of α-Sn, the value of k_r for α-Sn would appear to lie in the range $(8{\cdot}5 \text{ to } 12{\cdot}5) \times 10^4$ dyn/cm.

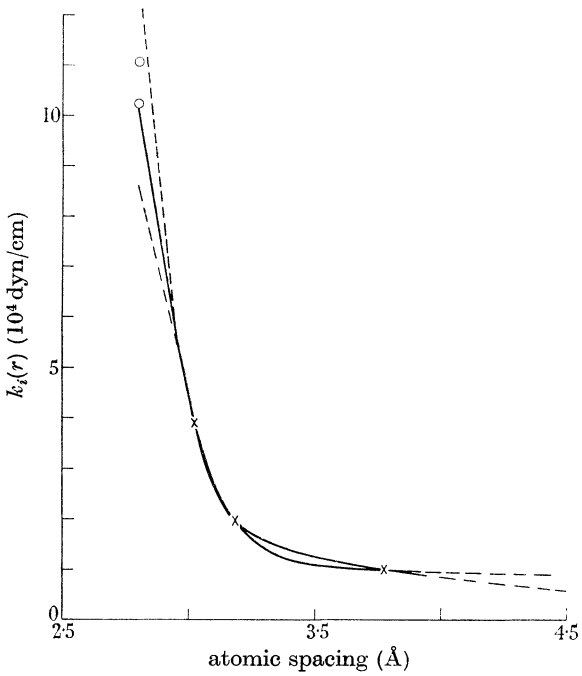

FIGURE 4. The extensional stiffnesses $k_i(r)$ $(i = 1, 2, 3)$ as a function of the atomic spacing r.

A better estimate of the constant c_{44} is possible by use of an expression for the Debye temperature at 0 °K, Θ_0, due to de Launay (1954). This gives

$$\Theta_0^3 = \frac{9N}{4\pi V}\left(\frac{h}{k}\right)^3\left(\frac{c_{44}}{\rho_D}\right)^{\frac{3}{2}}\frac{9}{18+\sqrt{3}}f(s,t), \tag{9·1}$$

where N is Avogadro's number,
V is the molar volume,
h is Planck's constant,
k is Boltzmann's constant,
ρ_D is density,
f is a tabulated function dependent on the elastic anisotropy of the crystal,

$$s = \frac{c_{11}-c_{44}}{c_{12}+c_{44}}, \quad t = \frac{c_{12}-c_{44}}{c_{44}}.$$

With the physical data for germanium available, $c_{44}^{\alpha\text{-Sn}}$ may be estimated from the expression

$$\frac{c_{44}^{\alpha\text{-Sn}}}{c_{44}^{\text{Ge}}} = \left(\frac{\rho_D^{\alpha\text{-Sn}}}{\rho_D^{\text{Ge}}}\right)\left(\frac{a^{\alpha\text{-Sn}}}{a^{\text{Ge}}}\right)\left(\frac{\Theta_0^{\alpha\text{-Sn}}}{\Theta_0^{\text{Ge}}}\right)^2\left(\frac{f^{\text{Ge}}}{f^{\alpha\text{-Sn}}}\right)^{\frac{2}{3}}, \tag{9·2}$$

derived from (9·1). The value of $\Theta_0^{\alpha\text{-Sn}}$ has been taken as 230 °K. This estimate was made by noting that, in the cases of silicon and germanium studied by Flubacher *et al.* (1959), the value of Θ_0 is very close to the maximum value observed at higher

temperatures; assuming a similar behaviour for grey tin, the analogous value for $\Theta_0^{\alpha\text{-Sn}}$, ⊕, was read off the curve derived from the observed specific heat, $C_v(T)$ in figure 7. The value of f^{Ge} is given by de Launay (1956) as 0·7095 and it is not

TABLE 4. FORCE CONSTANTS AND ELASTIC CONSTANTS FOR DIAMOND STRUCTURE ELEMENTS

Units: c_{ij} in 10^{11} dyn/cm², k_j in 10^4 dyn/cm.

element	$c_{11}+2c_{12}$	$c_{11}-c_{12}$	c_{44}	$\frac{c_{11}+2c_{12}}{c_{11}-c_{12}}$	k_r	k_θ	reference
C	173	56	43	3·09	61·6	3·17	Bhagavantam & Bhimasenachar
	132·6	95·1	57·5	1·40	47·2	5·62	McSkimin & Bond
Si	29·77	10·24	8·01	2·91	16·15	0·926	McSkimin
Ge	22·90	8·20	6·87	2·79	12·94	0·777	McSkimin
α-Sn	19·2	4·8	3·5	4·0	12·41	0·518	Potter
	17·07	5·69	3·94	3·0	11·08	0·616	present suggestions I
	15·75	5·25	3·64	3·0	10·23	0·568	present suggestions II

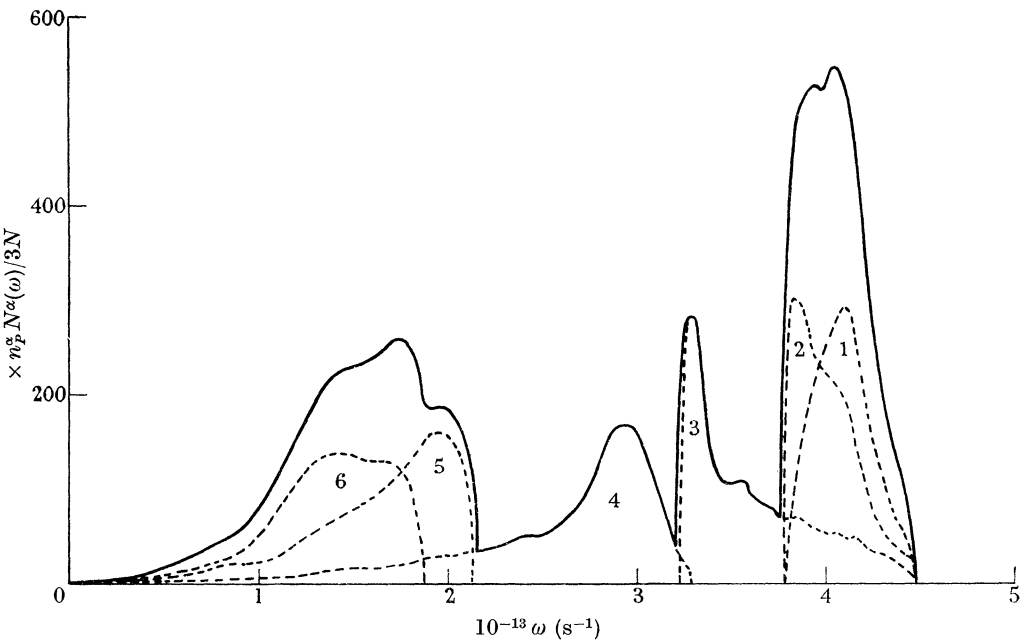

FIGURE 5. Calculated frequency distribution of lattice modes in α-Sn. n_P^α is the effective total population of calculated frequencies, $N^\alpha(\omega)\,\Delta\omega$ is the number of frequencies per mole lying in the range $\Delta\omega$. N is Avogadro's number.

unreasonable to suppose that $f^{\alpha\text{-Sn}}$ will take a similar value; however, for consistency with the proposed simple model with $k_r = 18k_\theta$, $s = \frac{38}{53}$, $t = -\frac{1}{27}$ and the corresponding value of $f^{\alpha\text{-Sn}}$ is then 0·803. Table 4 gives the various c_{ij} and k_j with the values proposed for α-Sn as f has the value 0·7095 (I) or 0·803 (II). It will be remarked that the proposed values of k_r are well inside the bounds suggested by the extrapolated curves of figure 4.

With the use of this latter set (II) of k_r and k_θ, the secular equation for diamond structure has been solved over a population of 89 wave vectors whose extremities are uniformly distributed over the repeating $\frac{1}{48}$ portion of the Brillouin zone. The resulting frequency distribution is shown in figure 5 and has been used to compute thermodynamic quantities for comparison with observed values in § 10.

10. Comparison of calculated and observed specific heats for α- and β-Sn

The frequency distributions for the two phases shown in figures 3 and 5 were obtained by plotting the density of modes for each branch using intervals of the form $\{\omega - 2h, \omega\}$, $\{\omega - h, \omega + h\}$, $\{\omega, \omega + 2h]$ and taking the mean of the three ordinates so found for the frequency ω; in calculating the ordinates, the contribution to the density by the frequencies for each wave vector was weighted in accordance with the symmetry of the repeating portion of the Brillouin zone; the total frequency distribution was obtained by adding the results for the branches.

Table 5. Calculated specific heats $C_v(T)$ as a function of temperature for the two phases of tin

	C_v (cal mole^{-1} deg K^{-1})	
T (°K)	α-Sn	β-Sn
5	—	0·0244
10	0·0383	0·1456
15	0·1399	0·4013
25	0·556	1·181
50	1·912	3·229
75	3·1316	4·322
100	3·9904	4·929
150	4·910	5·457
200	5·3245	5·667
250	5·542	5·768
300	5·657	5·825
400	5·729	5·884

The lattice contributions to the specific heat at constant volume per mole as a function of temperature, $C_v(T)$, were computed by numerical integration of the contributions from the modes indicated by the frequency distribution. The Einstein specific heat as a function of $\hbar\omega/kT$ according to the tables of Landolt & Börnstein (1927) was found for each frequency interval, was weighted by the appropriate ordinate of the frequency distribution and the sum of such contributions divided by the total number of modes.

The calculated values are given in table 5 and plots of the calculated and observed (Lange 1924) specific heats for the two phases are shown in figure 6.

It is clear that the calculated values significantly underestimate the specific heat even when allowance is made for the difference $C_p - C_v$ and electronic contributions. The former correction as estimated by Hill & Parkinson (1952) for α-Sn amounts to 2 % at 100 °K and will be of similar magnitude for β-Sn. The coefficient of the

linear term in the expansion of $C_v(T)$ attributable to electronic contribution has magnitude $\sim 10^{-4}$ cal mole^{-1} deg K^{-2}. Kittel (1956) quotes 4×10^{-4} cal mole^{-1} deg K^{-2} for β-Sn so that a correction of $\sim 0{\cdot}1$ cal mole^{-1} deg K^{-1} at 300 °K would be appropriate. Thus there remains a significant discrepancy between experimental and calculated values, particularly at lower temperatures, which is almost certainly due to the models of the structures being too stiff as a result of which the frequency distributions show maxima in the densities of modes at higher frequencies than those which are in fact most heavily populated by the phonons. Alternatively expressed, the Debye temperatures estimated from the calculated specific heats will be too high.

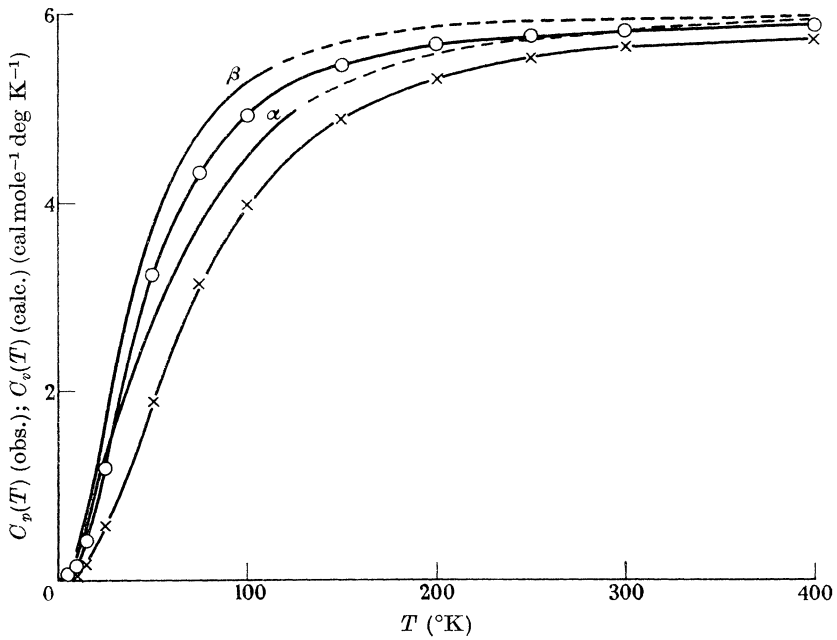

FIGURE 6. The calculated values of specific heat $C_v(T)$ for α-Sn (×) and β-Sn (○) compared with observed values of $C_p(T)$.

11. COMPARISON OF CALCULATED AND OBSERVED DEBYE TEMPERATURES

Values of $\Theta(T)$ may be estimated from the calculated and observed specific heats of the two phases and a comparison is shown in figure 7.

The discrepancies again emphasize the excessive stiffness of the models.

Both the force fields used have effectively been derived from the mechanical properties of β-Sn in the absence of other relevant data. The frequencies calculated for optical modes may be seriously inaccurate and will be those most affected by high values of short-range stiffnesses. Such overestimates will surely occur if the representation of the structure employs too short a range of interaction. It seems probable therefore, that the discrepancies in the calculated and observed thermal data are due to the model involving stiffnesses to short-range deformations which are too high.

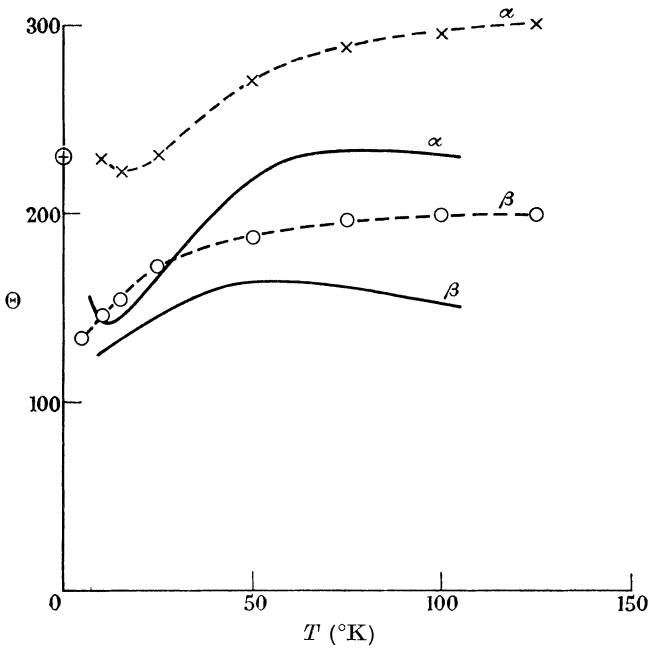

FIGURE 7. Characteristic temperatures $\Theta(T)$ derived from calculated (– – – –) and observed (——) specific heats of α-Sn and β-Sn.

12. COMPARISON OF THE FREE ENERGIES OF THE PHASES AND ESTIMATION OF THE TRANSITION TEMPERATURE

The frequency distributions may also be used to calculate the vibrational contributions to the free energies $F^{\alpha}_{\text{vib.}}(T)$, $F^{\beta}_{\text{vib.}}(T)$ of the two phases as a function of temperature. Landolt & Börnstein (1927) give values of

$$\frac{F_{\text{vib.}}(T)}{T} = \frac{1}{T}\int_0^T C_v(T)\,\mathrm{d}T - \int_0^T \frac{C_v(T)}{T}\,\mathrm{d}T, \tag{12·1}$$

as a function of $\hbar\omega/kT$. A comparison of the vibrational contributions $F_{\text{vib.}}(T)$ of the two phases is given in table 6.

TABLE 6. THE VIBRATIONAL CONTRIBUTIONS TO FREE ENERGY $F_{\text{vib.}}(T)$ (CAL/MOLE) AS A FUNCTION OF TEMPERATURE FOR THE TWO PHASES OF TIN

T (°K)	$-F^{\alpha}_{\text{vib.}}$	$-F^{\beta}_{\text{vib.}}$	$-[F^{\beta}_{\text{vib.}} - F^{\alpha}_{\text{vib.}}]$
50	15·455	34·885	19·43
100	116·42	209·68	93·26
150	315·63	509·30	193·67
200	597·38	899·18	301·80
250	945·95	1365·30	419·35
300	1350·15	1886·79	536·64
400	2293·04	3077·48	784·44

The relative stability of the phases is determined by the respective total free energies and an estimate of the transition temperature is obtained when the

difference in vibrational contributions is equal in magnitude but opposite in sign to the difference in internal energy at zero temperature, i.e.

$$E_0^\beta - E_0^\alpha = -[F_{\text{vib.}}^\beta(T) - F_{\text{vib.}}^\alpha(T)]. \tag{12·2}$$

The right-hand side of (12·2) is plotted as a function of temperature in figure 8. Seitz (1940) quotes the difference in internal energy at 0 °K as 399 cal/mole and hence from figure 8, we obtain 242 °K as a calculated estimate of the transition temperature; this may be compared with the observed result of 286 °K (Busch & Kern 1960). The relatively good agreement, in view of the assumptions involved in the formulation of the models, is due to the difference of specific heats for the two phases, as calculated and observed, being in better agreement than the absolute values for the individual phases.

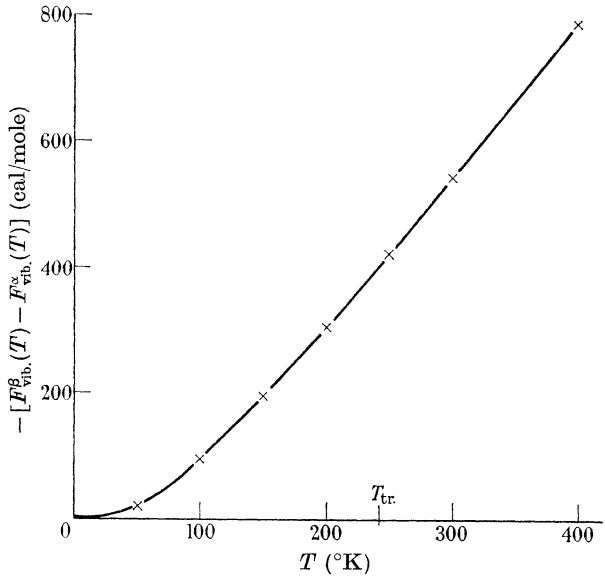

FIGURE 8. The difference in the vibrational contribution to the free energy of the two phases as a function of temperature calculated from the models. At the estimated transition temperature, 242 °K, this difference is equal in magnitude and opposite in sign to the difference in the internal energies at zero temperature.

13. THE STABILITY OF THE TRANSITIONAL STRUCTURES

The hypothesis latent in this work is that since the two forms of tin may both be regarded as body-centred tetragonal structures of different axial ratios, the transition between them might take place by means of a homogeneous shear of the type $(\frac{1}{2}\epsilon, \frac{1}{2}\epsilon, -\epsilon)$.

The expression for the shear constant which controls this deformation was given in (7·13) and related to the force constants and the axial ratio parameter ρ. It is interesting to enquire into the value of this constant as the value of ρ changes in the range $0{\cdot}272 < \rho < 0{\cdot}707$. This can be done by assuming a linear interpolation of first-neighbour distance over the range and then calculating the other spacings from the expressions of table 2. The curve in figure 4 then offers an estimate of the

point-to-point stiffness for any spacing. It is possible to put a value on $k_\phi(\rho)$ by interpolation between the values for α-Sn and β-Sn where it is reasonable to assume that the value for the symmetrical valence structure of α-Sn will be a maximum. Figures 9 (*a*) and (*b*) give the atomic spacings, $r(\rho)$ and the value of $k_\phi(\rho)$. We may now calculate all the terms in the expression for the shear constant

$$c_{11}+c_{12}-4c_{13}+2c_{33}$$

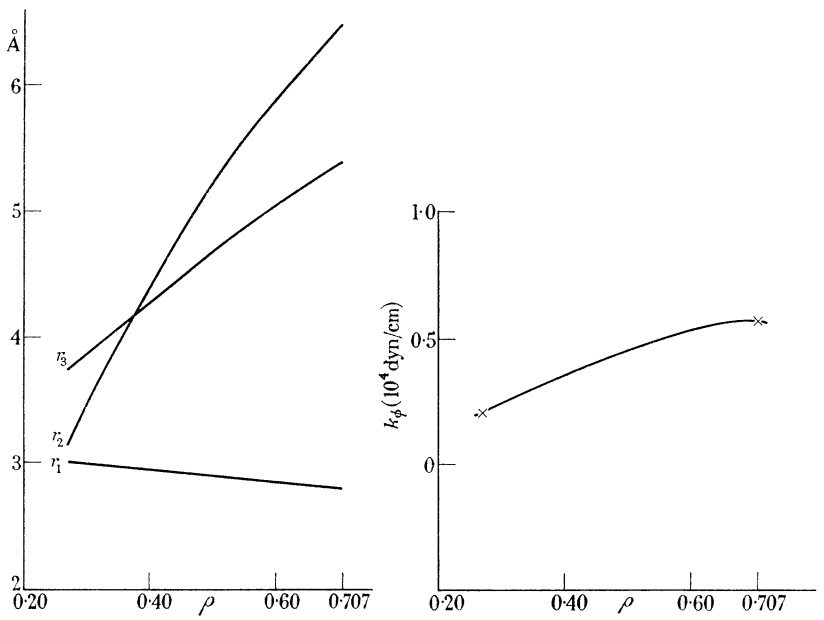

FIGURE 9. (*a*) Atomic spacings of first, second and third neighbours and (*b*) the force constant k_ϕ as functions of ρ.

TABLE 7. CONTRIBUTIONS OF THE ATOMIC STIFFNESSES TO THE SHEAR CONSTANT $c_{11}+c_{12}-4c_{13}+2c_{33}$

Units: k_j in 10^4 dyn/cm

ρ	A_1k_1	A_2k_2	A_3k_3	$A_\phi k_\phi$	ΣA_jk_j	$k_\phi^{+\text{crit.}}(=-\Sigma A_jk_j/A_{\phi'})$
0·272	0·658	1·163	0·017	0·017	1·855	−2·849
0·3	0·708	0·958	0·049	0·027	1·742	−2·345
0·4	0·563	0·728	0·253	0·105	1·649	−1·329
0·5	0·350	0·400	0·471	0·270	1·491	−0·626
0·6	0·122	—	0·443	0·529	1·094	−0·459
0·707	0	—	—	2·556 ($k_{\phi'}=k_\phi$)	2·556	

$$c_{11}+c_{12}-4c_{13}+2c_{33}=(4/c)\,[A_1k_1+A_2k_2+A_3k_3+A_\phi k_\phi+A_{\phi'}k_{\phi'}^+],$$

where

$$A_1=\frac{(1-2\rho^2)^2}{4(1+\rho^2)},\quad A_2=8\rho^2,\quad A_3=\frac{(1-18\rho^2)^2}{4(1+9\rho^2)};$$

$$A_\phi=\frac{18\rho^4}{(1+\rho^2)(1+2\rho^2)},\quad A_{\phi'}=\frac{9\rho^2}{1+\rho^2};$$

$k_{\phi'}^{+\text{crit.}}$ is the value of this force constant that makes $c_{11}+c_{12}-4c_{13}+2c_{33}=0$.

except that containing $k_{\phi'}+k_{\phi'\phi'}$ and these are itemized in table 7. There seems no way of estimating the values of $k_{\phi}^{\pm}(\rho)$; if the explanation of the calculated negative values, as offered in the next section, is qualitatively correct, there will occur a discontinuity as ρ is decreased from 0·707 and the value of $k_{\phi}^{\pm}$ will change from positive to negative. We may enquire, however, what value of $k_{\phi}^{\pm}$ is necessary to reduce the shear constant $c_{11}+c_{12}-4c_{13}+2c_{33}$, to zero and these critical values of $k_{\phi}^{\pm}$ are shown in the table. It is noteworthy that for $\rho = 0{\cdot}5$, 0·6, the values are not very large and indeed could render the structure unstable in this mode of shear before the onset of instability in the lattice modes of wave number $(2\pi/a', 0, 0)$; the condition for stability in such lattice modes is given by (A 2·2) and requires

$$k_{\phi'} > -0{\cdot}6207 \quad \text{and} \quad > -0{\cdot}9410$$

as $\rho = 0{\cdot}5$ and 0·6 respectively (cf. table 7). A further point of interest is that the interaction of second neighbours appears to be the principal stabilizing contribution to this shear stiffness.

14. Interpretation of the calculated values of the force constants

In attempts to calculate the elastic constants of a crystal from the fundamental ionic and electronic structure, the cohesive energy and its variation under strain are usually considered in three main parts. These are (1) the various electrostatic or Coulomb interactions, (2) the exchange interaction between ion cores, (3) the interaction of the Fermi surface with the Brillouin polyhedra of the structure. Of these, (1) and (2) may effectively be regarded as giving rise to central force fields, while (3) may not be so simply classified. Thus the force constants k_1, k_2, k_3 of this note may reasonably be associated predominantly with (1) and (2) while although positive point-to-point stiffnesses such as k_1, k_2, k_3 may imply a measure of angular stiffness, the large positive values of k_θ shown by the diamond structures (see table 4) and the large negative values of $k_{\phi'}$ and $k_{\phi'\phi'}$ (table 3) must be accounted for under (3).

Jones (1949) was the first to relate the geometry of a Fermi surface to the values of elastic shear constants. In considering the shear constants of β-brass, he suggested that significant contributions to these constants could be occasioned by the filling of the momentum states close to the planes of energy discontinuity. A shear strain in configuration space produces a corresponding shear in reciprocal space and this can result in an appreciable increase or decrease in the energy of the electrons as they occupy the states available under the strained condition. Broadly speaking, a positive contribution to the shear constant occurs when the Fermi surface is just contained by a plane of energy discontinuity and a negative contribution when the surface overlaps such a plane; the magnitudes of these contributions will be related to the energy gap. Jones found stabilizing contributions to the shear constants of β-brass while Leigh (1951) found destabilizing contributions to the shear constants of aluminium.

In consequence, it is tempting to attribute the positive values of k_θ found in the diamond structures with the containment of the occupied states by the fourth Brillouin zone, a rhombic dodecahedron across whose bounding faces there exists

an energy gap of decreasing magnitude with C, Si, Ge, α-Sn. Similarly, the negative values of $k_{\phi'}$ and $k_{\phi'\phi'}$, which tend to destabilize the β-Sn (or an intermediate) structure, may be qualitatively related to the overlap of the Fermi surface on some of the planes of Bragg reflexion for the structure. For example, an overlap of occupied states on Bragg planes which are parallel to the tetragonal axis, while unoccupied states exist within the same zone in the neighbourhood of the axis would offer a destabilizing contribution to any stiffness associated with a change of axial ratio, ρ; in the present case, $k_{\phi'}+k_{\phi'\phi'}$ is just such a stiffness and it is suggested that

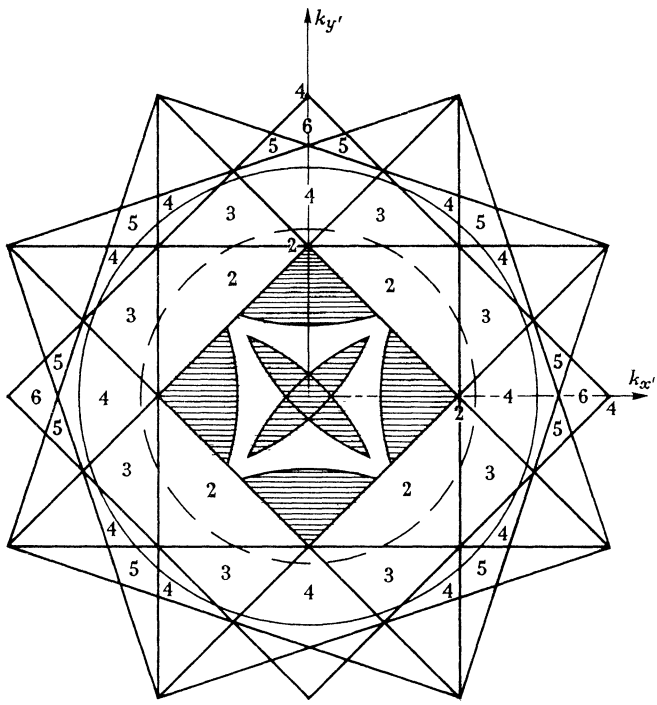

FIGURE 10. The (0, 0, 1) section of the Brillouin zones in momentum space. The circles show the trace of a Fermi sphere for $\rho = 1/\sqrt{2}$ (dashed line) and for $\rho = 0{\cdot}272$ (full line). The shaded areas in the first zone represent the filling of the fourth zone by the latter sphere on a reduced zone scheme as used by Gold & Priestley. The axes are marked in units of π/a'.

the negative values found are the result of the negative contribution from the Fermi electrons preponderating over any positive contributions. Overlap of the (2, 2, 0) planes has been suggested by Lee & Raynor (1954) in a consideration of the variation of axial ratio with electron concentration in tin alloys. More recently, Gold & Priestley (1960) have published a realization of the Fermi surface for white tin interpreted from de Haas–van Alphen measurements. This shows the Fermi surface to be very complicated and extending into the sixth Brillouin zone so that the prospects of making quantitative assessments of the contributions to the atomic or macroscopic stiffnesses appear remote. However, one distinctive feature of this complex surface is an overlap on (2, 2, 0) planes of the fourth zone in extended k-space. The (0, 0, 1) section of momentum space with the trace of the Fermi

sphere considered by Gold & Priestley is shown in figure 10. For a shear in the $x'y'$-plane in which the square section is distorted to a rectangle, $k_{\phi'}$ and $k_{\phi'\phi'}$ must contribute with opposite sign as appears in the expression for $c_{11}-c_{12}$, (7·12). This abatement of the negative contribution of these two force constants is perhaps related to the adjustment of states under strain taking place only over the Bragg planes parallel to the tetragonal axis.

During the transition from diamond ($\rho = 0{\cdot}707$) to white tin ($\rho = 0{\cdot}272$) structure, the radius of the Fermi sphere given by $(3/\pi\rho)^{\frac{1}{3}}\, 2\pi/a'$ effectively increases from $1{\cdot}106(2\pi/a')$ to $1{\cdot}518(2\pi/a')$. For diamond structure, the four electrons/atom are contained by the dodecahedral zone whose bounding section in the (0, 0, 1) plane is defined by the (± 2, 0, 0), (0, ± 2, 0) planes. The overlap indicated by the dashed circle does not occur until some electrons acquire sufficient energy to cross the gap when a destabilizing contribution to the shear mode controlling the axial ratio ρ is caused. It is suggested that this effect predominates for intermediate values of ρ until the stabilizing effect of the stiffness k_2 becomes sufficiently large.

15. Discussion

In this essay, an attempt has been made to relate the structures of grey and white tin in a simple mechanical way and on the basis of a lattice dynamical model to calculate thermodynamic quantities for the two phases and compare the results with experimental data. Considerable assumptions and some extensive extrapolation have been involved but the final comparison with experimental thermal data is not unfavourable to the main hypotheses of the discussion. However, the basic ideas are little more than intuitive and their validity may well be questioned.

In particular, the choice of the force field for the model is open to criticism on the one hand from experts in band structure for whom a model for a metallic structure based on the interaction of close neighbours may be anathema and on the other from molecular spectroscopists who may be disturbed by the negative value of a principal angular stiffness. That the model is inadequate is all too clearly the case; how should it be otherwise when determined by six physical constants? However, to the former group of critics, it is perhaps pertinent to suggest that although the equations of motion include only selected interactions up to sixth neighbours, the interpretation of angular stiffness is in terms of concepts dependent on the periodicity of the structure. To the latter group, the extent to which the force constants require modification in order to achieve stability may be a measure of the model's inadequacy; however, in an attempt to represent two structures in conditions near instability, it is an embarrassing but not altogether unhealthy feature to find a parameter, which is closely associated with the mode of instability, extremely sensitive.

Finally, it is appropriate to point out that the section on the structures of intermediate values of the axial ratio takes even more for granted than the remainder; for, in effect, use is made of small deflexion theory when undeniably the deflexions from either equilibrium state are large and constraints would be necessary to achieve a pseudo-equilibrium for such states.

The mechanics of the transition between the phases of tin is believed to be

highly relevant to the transitions observed when other diamond structure elements and zinc-blende compounds are subjected to hydrostatic pressure (Minomura & Drickamer 1962; Samura & Drickamer 1962; Jayaranam *et al.* 1961; Gebbie *et al.* 1960)). Here again a proper treatment requires a theory of large deflexions but it is hoped that the present essay will contribute to the understanding of these phase changes.

I wish to thank Dr A. J. Leadbetter for drawing my attention to de Launay's expression (9·1) as a means of estimating, c_{44} for α-Sn. I would further acknowledge with appreciation many encouraging discussions with Mr H. L. Cox; also the unfailing assistance of Miss P. Noyes, Basic Physics Division, who prepared the figures and tables, did much tedious hand computation and, with the help of Miss B. Webber and other staff of Mathematics Division, dealt with the progress of the computations performed on ACE.

This work has formed part of the research programme of the National Physical Laboratory and is published with the permission of the Director.

References

Bhagavantam, S. & Bhimasenachar, J. 1946 *Proc. Roy. Soc.* A, **187**, 381.
Born, M. & Huang, K. 1956 *The dynamics of crystal lattices.* Oxford University Press.
Bridgman, P. W. 1925 *Proc. Amer. Acad. Arts Sci.* **60**, 305.
Busch, G. A. & Kern, R. 1960 *Solid State Phys.* vol. 11. New York: Academic.
Ewald, A. W. & Tufte, O. N. 1958 *J. Appl. Phys.* **29**, 1007.
Flubacher, P., Leadbetter, A. J. & Morrison, J. A. 1959 *Phil. Mag.* **4**, 273.
Gebbie, H. A., Smith, P. L., Austin, I. G. & King, J. H. 1960 *Nature, Lond.* **188**, 1095.
Gold, A. V. & Priestley, M. G. 1960 *Phil. Mag.* **5**, 1089.
Hall, E. O. 1956 *The mechanism of phase transformations in metals.* Institute of Metals Symposium.
Hill, R. W. & Parkinson, D. H. 1952 *Phil. Mag.* **43**, 309.
House, D. G. & Vernon, E. V. 1960 *Brit. J. Appl. Phys.* **11**, 254.
Jayaranam, A., Kennedy, G. C. & Newton, R. C. 1961 *Nature, Lond.* **191**, 1288.
Jones, H. 1952 *Phil. Mag.* **43**, 105.
Kittel, C. 1956 *Introduction to solid state physics.* New York: Wiley.
Landolt, H. & Börnstein, R. 1927 *Phys.-Chem. Tabellen.* §265A. Berlin: Springer.
Lange, F. 1924 *Phys. Chem.* **110**, 343.
Launay, J. de 1954 *J. Chem. Phys.* **22**, 1676.
Launay, J. de 1956 *Solid State Phys.* **2**, 219.
Lee, J. A. & Raynor, G. V. 1954 *Proc. Phys. Soc.* B, **67**, 737.
Leigh, R. S. 1951 *Phil. Mag.* **42**, 139.
Mason, W. P. & Bömmel, H. E. 1956 *J. Acoust. Soc. Amer.* **28**, 930.
McSkimin, H. J. 1953 *J. Appl. Phys.* **24**, 988.
McSkimin, H. J. & Bond, W. L. 1957 *Phys. Rev.* **105**, 116.
Miasek, M. & Suffczynski, M. 1961 *Bull. Acad. Polon. Sci.* **9**, 447.
Minomura, S. & Drickamer, H. G. 1962 *J. Phys. Chem. Solids*, **23**, 451.
Musgrave, M. J. P. & Pople, J. A. 1962 *Proc. Roy. Soc.* A, **268**, 474.
Potter, R. F. 1957 *J. Phys. Chem. Solids*, **3**, 223.
Prasad, S. C. & Wooster, W. A. 1956 *Acta Cryst.* **9**, 35.
Rayne, J. A. & Chandrasekhar, B. S. 1960 *Phys. Rev.* **120**, 1658.
Samara, G. A. & Drickamer, H. G. 1962 *J. Phys. Chem. Solids*, **23**, 457.
Seitz, F. 1940 *The modern theory of solids.* New York: McGraw Hill.
Wolfson, R. G., Fine, M. E. & Ewald, A. W. 1960 *J. Appl. Phys.* **31**, 1973.
Wyckoff, G. G. 1948 *Crystal structures.* New York: Academic.

Appendix 1. The dynamical matrices for the sets of interacting neighbours

1st neighbours

$$\left.\begin{aligned}
\Phi_{\alpha\beta}(1,\bar{1}) &= -\begin{bmatrix} \beta & 0 & -\gamma \\ 0 & \alpha & 0 \\ -\gamma' & 0 & \beta' \end{bmatrix}, \quad \Phi_{\alpha\beta}(1,\bar{2}) = -\begin{bmatrix} \beta & 0 & \gamma \\ 0 & \alpha & 0 \\ \gamma' & 0 & \beta' \end{bmatrix} \\
\Phi_{\alpha\beta}(1,\bar{3}) &= -\begin{bmatrix} \alpha & 0 & 0 \\ 0 & \beta & \gamma \\ 0 & \gamma' & \beta' \end{bmatrix}, \quad \Phi_{\alpha\beta}(1,\bar{4}) = -\begin{bmatrix} \alpha & 0 & 0 \\ 0 & \beta & -\gamma \\ 0 & -\gamma' & \beta' \end{bmatrix}
\end{aligned}\right\} \quad \text{(A 1·1)}$$

2nd neighbours

$$\left.\begin{aligned}
\Phi_{\alpha\beta}(1,14) &= -\begin{bmatrix} \delta & 0 & 0 \\ 0 & \delta' & 0 \\ 0 & 0 & \delta'' \end{bmatrix}, \quad \Phi_{\alpha\beta}(1,16) = -\begin{bmatrix} \delta' & 0 & 0 \\ 0 & \delta & 0 \\ 0 & 0 & \delta'' \end{bmatrix}
\end{aligned}\right\} \quad \text{(A 1·2)}$$

3rd neighbours

$$\left.\begin{aligned}
\Phi_{\alpha\beta}(1,\overline{12}) &= -\begin{bmatrix} \lambda & 0 & 0 \\ 0 & \mu & -\nu \\ 0 & -\nu' & \mu' \end{bmatrix}, \quad \Phi_{\alpha\beta}(1,\overline{13}) = -\begin{bmatrix} \lambda & 0 & 0 \\ 0 & \mu & \nu \\ 0 & \nu' & \mu' \end{bmatrix} \\
\Phi_{\alpha\beta}(1,\overline{14}) &= -\begin{bmatrix} \mu & 0 & \nu \\ 0 & \lambda & 0 \\ \nu' & 0 & \mu' \end{bmatrix}, \quad \Phi_{\alpha\beta}(1,\overline{15}) = -\begin{bmatrix} \mu & 0 & -\nu \\ 0 & \lambda & 0 \\ -\nu' & 0 & \mu' \end{bmatrix}
\end{aligned}\right\} \quad \text{(A 1·3)}$$

4th neighbours

$$\left.\begin{aligned}
\Phi_{\alpha\beta}(1,3) &= -\begin{bmatrix} \rho & \omega & \tau \\ \omega' & \rho' & \sigma \\ \tau' & \sigma' & \rho'' \end{bmatrix}, \quad \Phi_{\alpha\beta}(1,4) = -\begin{bmatrix} \rho & -\omega & \tau \\ -\omega' & \rho' & -\sigma \\ \tau' & -\sigma' & \rho'' \end{bmatrix} \\
\Phi_{\alpha\beta}(1,6) &= -\begin{bmatrix} \rho' & \omega' & -\sigma \\ \omega & \rho & -\tau \\ -\sigma' & -\tau' & \rho'' \end{bmatrix}, \quad \Phi_{\alpha\beta}(1,7) = -\begin{bmatrix} \rho' & -\omega' & -\sigma \\ -\omega & \rho & \tau \\ -\sigma' & \tau' & \rho'' \end{bmatrix} \\
\Phi_{\alpha\beta}(1,9) &= -\begin{bmatrix} \rho & \omega & -\tau \\ \omega' & \rho' & -\sigma \\ -\tau' & -\sigma' & \rho'' \end{bmatrix}, \quad \Phi_{\alpha\beta}(1,10) = -\begin{bmatrix} \rho & -\omega & -\tau \\ -\omega' & \rho' & \sigma \\ -\tau' & \sigma' & \rho'' \end{bmatrix} \\
\Phi_{\alpha\beta}(1,12) &= -\begin{bmatrix} \rho' & \omega' & \sigma \\ \omega & \rho & \tau \\ \sigma' & \tau' & \rho'' \end{bmatrix}, \quad \Phi_{\alpha\beta}(1,13) = -\begin{bmatrix} \rho' & -\omega' & \sigma \\ -\omega & \rho & -\tau \\ \sigma' & -\tau' & \rho'' \end{bmatrix}
\end{aligned}\right\} \quad \text{(A 1·4)}$$

6th neighbours

$$\left.\begin{aligned}
\Phi_{\alpha\beta}(1,2) &= -\begin{bmatrix} \zeta & 0 & \eta \\ 0 & \zeta' & 0 \\ \eta' & 0 & \zeta'' \end{bmatrix}, \quad \Phi_{\alpha\beta}(1,5) = -\begin{bmatrix} \zeta & 0 & -\eta \\ 0 & \zeta' & 0 \\ -\eta' & 0 & \zeta'' \end{bmatrix} \\
\Phi_{\alpha\beta}(1,8) &= -\begin{bmatrix} \zeta' & 0 & 0 \\ 0 & \zeta & \eta \\ 0 & \eta' & \zeta'' \end{bmatrix}, \quad \Phi_{\alpha\beta}(1,11) = -\begin{bmatrix} \zeta' & 0 & 0 \\ 0 & \zeta & -\eta \\ 0 & -\eta' & \zeta'' \end{bmatrix}
\end{aligned}\right\} \quad \text{(A 1·5)}$$

For the reference atom in the second lattice $\bar{1}$

$$\Phi_{\alpha\beta}(1,\bar{n}) = \Phi_{\beta\alpha}(\bar{1},n).$$

Appendix 2. The secular equation yielding the lowest root

As mentioned in § 8, initial computations using force constants derived directly from observed elastic constants of β-Sn yielded a small proportion of negative roots for $m\omega^2$ thereby indicating that the model was unstable.

In order to ensure the stability of the model in future computations, the values of the force constants obtained from elastic constants with modified values of c_{13} were used to find the lowest value of $m\omega^2$ to check that it was positive.

The secular equation with $(q_1 a', q_2 a', q_3 c) = (2\pi, 0, 0)$ gave the lowest root and it may be seen from (6·2) to (6·12) that the only non-zero elements of the determinant are

$$\left.\begin{aligned} F &= \frac{2[k_1+4\rho^2 k_\phi]}{1+\rho^2} + 8k_\phi + \frac{2k_3}{1+9\rho^2} - \frac{16\rho^2 k_\phi}{1+2\rho^2} = G, \\ H &= \frac{4[\rho^2 k_1 + 4\bar{k}_{\phi'}]}{1+\rho^2} + \frac{36\rho^2 k_3}{1+9\rho^2} + \frac{16}{1+\rho^2}\left\{\frac{\rho^2 k_\phi}{1+2\rho^2} + k_{\phi'\phi'}\right\} \\ &= \frac{4[\rho^2 k_1 + 4k_{\phi'}]}{1+\rho^2} + \frac{36\rho^2 k_3}{1+9\rho^2} + \frac{16\rho^2 k_\phi}{(1+\rho^2)(1+2\rho^2)}, \\ P &= \frac{2[k_1+4\rho^2 k_\phi]}{1+\rho^2} - 8k_\phi + \frac{2k_3}{1+9\rho^2} = -Q. \end{aligned}\right\} \tag{A 2·1}$$

The smallest roots are $m\omega^2 = H$ (twice), so that for stability

$$H > 0. \tag{A 2·2}$$

It is interesting and possibly significant that the associated displacement vectors are parallel to the tetragonal axis. Thus the lattice modes closest to instability have transverse character related to the shear which changes the axial ratio ρ. In fact, the angles ϕ' subtended at each atom are deformed by equal amounts, with the same or opposite sense, as the atom is a member of one or other Bravais lattice. Clearly, these are modes for which negative $k_{\phi'}$ will offer a significant destabilizing effect.